A TRM-Based Compatible Strengthening Solution for Rammed Earth Heritage: Investigation of the Bond Behavior

Antonio Romanazzi(✉), Daniel V. Oliveira, and Rui A. Silva

ISISE, University of Minho, Guimarães, Portugal
aromanazzi89@gmail.com,
{danvco, ruisilva}@civil.uminho.pt

Abstract. Raw earth is among the most ancient building materials and the related building techniques are found widespread around the world. Currently, it is estimated that about 25% of the global population lives in earthen buildings and about 10% of the UNESCO World Heritage is built with earth. Nevertheless, an important overlap can be observed when the geographical distribution of raw earth constructions is compared with that of the seismic hazard. This circumstance, combined with the seismic vulnerability of earthen buildings, results in a high seismic risk, as demonstrated by recent moderate earthquakes. Despite the current awareness for this problem, little has been done so far to develop proper strengthening solutions for the rammed earth heritage. Based on the effectiveness of externally bonded fibers for masonry buildings, the strengthening of rammed earth walls with an earth mortar coating reinforced with a geomesh is here adopted as a compatible solution. The objective of this work is to investigate and characterize the bond behavior of the above mentioned strengthening solution to further describe the response of the interaction mortar-mesh. To this purpose, an experimental program was undertaken based on a series of pull-out tests. Specimens were prepared using earth mortar, two different types of meshes (glass fiber and nylon) and considering different bonded lengths. The results highlighted distinct bond behaviors. In the case of the glass fiber mesh, the bond was granted by friction and mechanical interlocking, while the mechanical anchorage promoted by the transversal yarns granted the bond of the nylon mesh.

Keywords: Rammed earth · Compatible strengthening
Textile reinforced mortar · Pull-out test · Bonded length

1 Introduction

Raw earth is one of the most ancient building materials and its related building techniques are the most widespread in the world. Indeed, it is estimated that about one fourth of the global population lives in earthen constructions and about 10% of UNESCO World Heritage is built with earth [1]. The different building techniques based on the use of raw earth have been developed by different cultures, depending on the locally available materials, the type of earth and the background knowledge. Thus,

R. Aguilar et al. (Eds.): *Structural Analysis of Historical Constructions*,
RILEM Bookseries 18, pp. 1594–1602, 2019.
https://doi.org/10.1007/978-3-319-99441-3_171

it is possible to identify the use of adobe in the Latin-America region, in the Mediterranean basin, in Africa and part of Middle-Est and Oriental countries [2–4]. Regarding the rammed earth technique, it has been developed from various cultures (Asia, South America, Mediterranean basin, etc.) during different historical periods [1, 5]; an example is the Great Wall of China, whose construction started about twenty-four centuries ago with long sections built in rammed earth, or the Horyuji Temple in Japan whose rammed earth walls are dated back to twelve centuries ago [6].

In the Iberian Peninsula rammed earth is evidenced to have been used before the 7th century [7]. An important overlap can be observed when the geographical distributions of the seismic hazard, raw earth construction and global population density are compared. This circumstance, combined with the recognized high seismic vulnerability of the earthen buildings, results in a high seismic risk, as demonstrated by several calamities caused by recent earthquakes (e.g. Bam 2001, Pisco 2007 and Maule 2010) [8]. Thus, in order to decrease the seismic risk, the main action is the reduction of the seismic vulnerability of earthen heritage. Based on the effectiveness of externally bonded fibers (also known as textile reinforced mortar - TRM) applied to masonry buildings [9–11], the use of earth mortar coatings reinforced with geomeshes, as a compatible strengthening technique for rammed earth buildings, represents a reliable solution. This solution is composed of an inorganic matrix, whose role is to fix the fibers, confer compressive strength and grant geometrical stability to the composite, and of a grid, which provides tensile strength and capacity to distribute the forces through adhesion and friction within the matrix [9, 12].

The TRM technique for adobe has been widely studied in Peru with the use of low cost synthetic meshes [13], where it has been shown to provide enhanced structural ductility [14, 15]. Research on the strengthening of rammed earth buildings with TRM started recently and the first outcomes have shown improvement of the overall seismic capacity, similar to that obtained in the case of adobe [16]. Nevertheless, the few research conducted so far lacks a comprehensive approach on the strengthening system, as the global performance of the intervention is the main aspect addressed. In fact, the local behavior, which represents the starting point to predict the response of the strengthened structure, is overlooked. Furthermore, insufficient attention has been paid to the compatibility of the strengthening system, which is required to ensure effectiveness and durability of interventions [17]. Thus, in order to define the local response of TRM technique, the characterization of each component and of their interaction is fundamental. Thus, an experimental program was undertaken within the framework of the research project SafEarth, and the latest results are presented in this paper. Firstly, the mechanical properties of the component materials were characterized, which included a selected earth mortar, and a glass fiber mesh and a nylon mesh acquired both from a local supplier. Then, the interaction between the meshes and the mortar were investigated by means of a series of pull-out tests, considering different bonded lengths.

2 Experimental Program

2.1 Characterization of the Mortar

To manufacture the earth mortar, the soil characterized in a previous investigation [18] was sieved through a 2 mm aperture mesh and corrected by addition of sand in weight ratio of 1:2 (soil: sand) [2]. The water content for the optimal workability of the earth mortar was defined through the flow table test, as suggested by Gomes et al. [19], resulting in a value of 18%. The mechanical properties of the mortar were characterized by means of three-point bending tests and compression tests, performed according to EN 1015-11 [20] after a drying period of 28 days under constant climatic conditions (T = 20 ± 2 °C and RH = 60 ± 5%). The Young's modulus was assessed through compression test of four cylinders with ± 90 mm of diameter and ± 175 mm of height. After a drying period of 28 days (T = 20 ± 2 °C and RH = 60 ± 5%), the specimens were tested under monotonic displacement controlled (1.5 μm/s) and the deformations were recorded by three LVDTs set in the middle third. The results are presented in Table 1 in terms of particle size distribution, density (ρ), bending strength (f_b), compressive strength (f_c) and elastic modulus (E). The mechanical properties of earth mortar are comparable with those of rammed earth; indeed, according to the literature, the compressive strength of rammed earth walls is in the range 1–1.26 MPa [21, 22] and the Young's modulus is around 4200 MPa [23, 24]. Thus, the mechanical compatibility between the support and the matrix is ensured.

Table 1. Properties of the earth mortar (the coefficient of variation is reported inside parenthesis).

Clay (%)	Silt (%)	Sand (%)	ρ (g/cm^3)	f_c (MPa)	f_b (MPa)	E (MPa)
11	14	75	1.81 (1%)	1.17 (12%)	0.47 (14%)	4915 (20%)

2.2 Characterization of the Meshes

The characterization of the meshes, namely the glass fiber mesh (GM) and the nylon mesh (NM), addressed the mass per unit area (GSM), tensile strength and price per unit area. Following the standard ISO 3374 [25], the mass per unit area resulted in 93 g/m^2 and 63 g/m^2 for the glass fiber mesh and nylon mesh, respectively. The tensile strength was assessed according to ASTM D6637 [26] and RILEM TC-250 CSM [27]. Five specimens with 5 cm width and variable length (300 mm for GM and 200 mm for NM) were examined for each type of mesh. The samples were tested under monotonic displacement controlled (10 μm/s for GM and 100 μm/s for NM) along the main direction and the respective maximum linear force ($F_{w,Max}$), the elastic stiffness in the range 10–25% $F_{w,max}$ (E_1), 25–50% $F_{w,Max}$ (E_2) and 10–50% $F_{w,Max}$ (E_3) were computed (see Table 2). The results highlight the different stiffness and tensile strength of the two meshes. Although, the peak strain (ε_{peak}) of the nylon mesh might result excessive with respect to the strain capacity of rammed earth, both meshes seem to be appropriate for their strengthening. Indeed, in the case of an earthquake, too stiff and

too strong materials commonly used in civil interventions are not compatible with the deformations levels required from existing rammed earth buildings, thus making unsuccessful their structural contribution.

Table 2. Properties of meshes (the coefficient of variance is reported inside parenthesis).

	Price (€/m^2)	Mesh size (mm × mm)	GSM (g/m^2)	$F_{w,Max}$ (kN/m)	ε_u (mm/m)	ε_{peak} (mm/m)	E_1 (kN/m)	E_2 (kN/m)	E_3 (kN/m)
GM	0.85	8 × 9	93	18.4 (11%)	22 (10%)	21 (11%)	963 (9%)	933 (6%)	943 (6%)
NM	0.63	16 × 21	63	4.3 (2%)	500 (8%)	489 (8%)	24 (2%)	18 (6%)	20 (5%)

2.3 Characterization of the Interaction Mortar-Mesh (Pull-Out Tests)

To investigate the interaction between the mortar and the embedded mesh, pull-out tests were carried out considering different bonded lengths, namely 30 mm, 50 mm, 90 mm and 150 mm in the case of the glass fiber mesh, and 15 mm, 20 mm, 30 mm, 50 mm and 70 mm in the case of the nylon mesh. Each specimen consisted of a mortar cylinder with diameter of ± 150 mm and height corresponding to the bonded length. For each bonded length, five specimens were manufactured guaranteeing the correct filling of the mould and position of a single mesh band with 50 mm width. The drying of the specimens occurred for a period of 28 days under constant climatic conditions (T = 20 ± 2 °C and RH ± 60 ± 5%), after which they were subjected to displacement controlled pull-out tests. Different testing speeds were used for the glass fiber and nylon meshes, respectively, 10 μm/s and 50 μm/s. The displacements of the mesh were recorded by means of one LVDT set at the free end, and of two LVDTs set at the loaded end and as close as possible to the mortar surface (Fig. 1a). The results were analyzed in terms of maximum linear force referred to the width of the mesh ($F_{w,Max}$) and type of failure, since three types of failure modes were observed (Fig. 1b): (1) tensile failure in a dry (exterior) section of the mesh, (2) tensile failure in an embedded section of mesh and (3) slipping of the mesh.

In the case of the glass fiber mesh, the bonded length and the maximum linear force seem to show a bilinear relationship, as indicated in Fig. 2a. For the bonded length of 30 mm, failure occurred due to sliding of the mesh inside the mortar and without full exploitation of its tensile capacity (failure mode 3) (see Table 3). For the following bonded lengths, failure occurred due to rupture of an embedded mesh section (failure mode 2) (see Table 3), but the full exploitation of the tensile strength of the mesh was not achieved in any case. Furthermore, the maximum linear force is shown to increase with the bonded length up to 90 mm. After this point, the maximum linear force seems to attain a constant value.

The fact that the tensile strength of the mesh is not fully exploited is probably a consequence of damage occurring in the mesh due to its interaction with mortar. For instance, the yarns of the glass fiber mesh are constituted by bundles of fibers, but only the perimetral ones interact directly with the mortar and transfer the load to the core

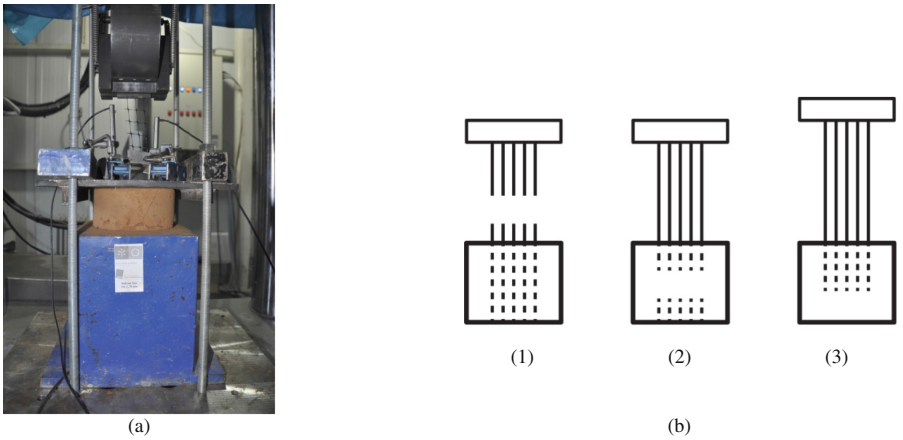

Fig. 1. Pull-out tests: (a) test setup; (b) observed failure modes.

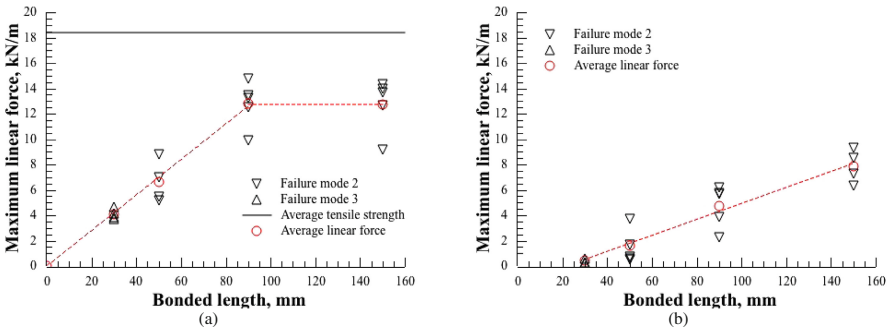

Fig. 2. Results of the pull-out tests of the glass fiber mesh: (a) correlation between the bonded length and the maximum linear force; (b) correlation between the bonded length and the linear force required to initiate sliding at the free-end.

Table 3. Results of pull-out tests of the glass fiber mesh.

Spec.	$F_{w,Max}$ (kN/m)	F. M.	Spec.	$F_{w,Max}$ (kN/m)	F. M.	Spec.	$F_{w,Max}$ (kN/m)	F. M.	Spec.	$F_{w,Max}$ (kN/m)	F. M.
G30_1	4.6	(3)	G50_1	6.9	(2)	G90_1	13.2	(2)	G150_1	14.4	(2)
G30_2	[a]	[a]	G50_2	5.2	(2)	G90_2	12.5	(2)	G150_2	13.7	(2)
G30_3	3.7	(3)	G50_3	[a]	[a]	G90_3	9.9	(2)	G150_3	12.7	(2)
G30_4	3.8	(3)	G50_4	5.4	(2)	G90_4	13.4	(2)	G150_4	14.0	(2)
G30_5	4.2	(3)	G50_5	8.8	(2)	G90_5	14.8	(2)	G150_5	9.2	(2)
Mean	4.1		Mean	6.6		Mean	12.8		Mean	12.8	
CoV	10%		CoV	25%		CoV	14%		CoV	17%	

[a]Failure of the mortar.

fibers. The perimetral fibers are likely to fray as slipping initiates, leading the yarns to rupture. In fact, the friction and the mechanical interlocking between the yarns and the mortar are deemed to be the main bond mechanism once sliding initiates. Figure 2b shows that the correlation between the average linear force required to onset the sliding at the free-end and the bonded length is apparently linear. Nevertheless, these values of the linear force are inferior to the respective maximum values, meaning that the sliding of the yarns activates an improved bond configuration. Furthermore, sliding of the mesh may occurs in different extents with respect to the yarns, meaning that the yarns are likely to achieve uneven stress levels. Overstressed yarns are also likely to lead to premature failure of the debilitated embedded mesh.

The results of the pull-out tests performed for the nylon mesh are presented in Fig. 3 and Table 4. In this case, the bonded length seems to have small influence on the maximum linear force, since the obtained values are similar to the tensile capacity of the mesh. In all cases, failure occurred due to rupture of the mesh in a section outside the mortar (failure mode 1) and no sliding at the free-end was observed, as expected. Thus, it can be stated that the tensile capacity of the nylon mesh was practically fully exploited independently from the bonded length. The bond of the mesh to the mortar was mainly granted by the mechanical anchoring mechanism promoted by the transversal yarns. It should be noted that each yarn of the nylon mesh is constituted by a single fiber and that the longitudinal and transversal yarns are bonded by plastic welded nodes. Furthermore, the embedding of a single transversal yarn (case of the 15 mm and 20 mm bonded lengths) was found to create sufficient bond to exploit the tensile capacity of the mesh.

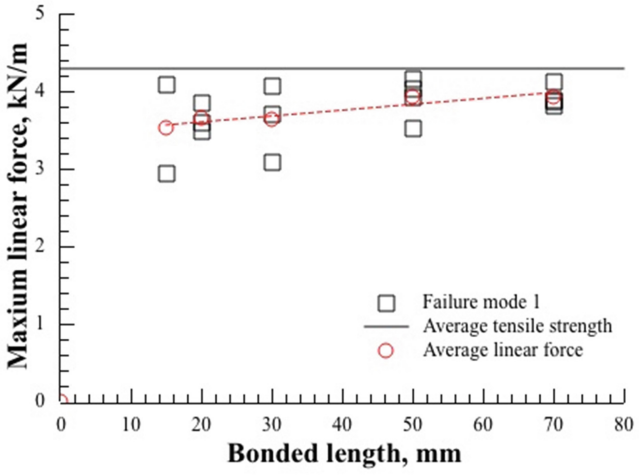

Fig. 3. Correlation between the bonded length and the maximum linear force for the nylon mesh

Table 4. Results of pull-out tests of the nylon mesh.

Spec.	$F_{w,Max}$ (kN/m)	F. M.	Spec.	$F_{w,Max}$ (kN/m)	F. M.	Spec.	$F_{w,Max}$ (kN/m)	F. M.	Spec.	$F_{w,Max}$ (kN/m)	F. M.	Spec.	$F_{w,Max}$ (kN/m)	F. M.
N15_1	2.9	(1)	N20_1	3.9	(1)	N30_1	4.1	(1)	N50_1	4.2	(1)	N70_1	3.9	(1)
N15_2	[a]	[a]	N20_2	[a]	[a]	N30_2	3.7	(1)	N50_2	3.9	(1)	N70_2	3.9	(1)
N15_3	4.1	(1)	N20_3	3.6	(1)	N30_3	3.1	(1)	N50_3	3.5	(1)	N70_3	4.1	(1)
N15_4	[a]	[a]	N20_4	[a]	[a]				N50_4	4.0	(1)	N70_4	3.8	(1)
			N20_5	3.5	(1)				N50_5	3.9	(1)			
Mean	3.5		Mean	3.7		Mean	3.6		Mean	3.9		Mean	3.9	
CoV	–		CoV	5%		CoV	14%		CoV	6%		CoV	3%	

[a]Failure of the mortar.

3 Conclusions

This paper presents the first experimental results on the investigation of the local behavior of a proposed TRM-based compatible strengthening solution for rammed earth constructions. In particular, the two components, namely the earth mortar and meshes, and their interaction were investigated through an experimental program.

The mortar showed compressive and tensile strength values similar to those of rammed earth, which contributes to promote mechanical compatibility between the matrix and the support, ensuring collaboration between the two elements and avoiding differentiated distribution of stresses.

The glass fiber mesh and nylon mesh presented mass per unit area appropriate for their use in composite materials, but their behavior was found to be substantially different. The glass fiber mesh showed much higher stiffness and tensile strength than those of the nylon mesh. In this last case, the low stiffness may represent an issue, since large deformations are required to fully develop the tensile strength of the mesh. Although their different behavior, both meshes are deemed to represent interesting solutions to enhance the structural ductility of rammed earth walls.

The pull-out tests revealed distinct interaction responses between the earth mortar matrix and the meshes. In the case of the glass fiber mesh, the tensile rupture of the embedded section of the mesh was the observed failure mode for the bonded lengths of 50 mm, 90 mm and 150 mm, while sliding failure was observed for the bonded length of 30 mm. The maximum linear force was shown to increase with the bonded length up to 90 mm and seems remain constant after this value (bilinear relationship). Furthermore, it was found that full exploitation of the tensile strength of the mesh was not possible probably due to damage resulting from the interaction between the mortar and the mesh.

In the case of nylon mesh, the maximum linear force values achieved by all bonded lengths tested were similar to the tensile strength of the mesh, and the failure occurred at an exterior section of the mesh. In fact, the embedding of a single transversal yarn was found to provide sufficient mechanical anchorage to fully exploit the tensile strength of the nylon mesh. This behavior results from the fact that the longitudinal and transversal yarns of this mesh are plastic welded at the intersection nodes and that the mesh presents low tensile strength values.

Finally, it can be concluded that the bond behavior of the glass fiber mesh is governed by the friction and mechanical interlocking with the mortar, while that of the nylon mesh is governed by the mechanical anchorage promoted by the transversal yarns. Furthermore, it should be noted that the investigation of the local behavior of the proposed TRM-based compatible strengthening solution should continue with the characterization of the bond stress-strain law at the mortar-mesh interface. Also, the interaction between the composite mesh-mortar system and the rammed earth substrate requires to be studied. In this regard, a subsequent experimental program is being prepared, where single-lap shear tests and diagonal compression tests are expected to be carried out.

Acknowledgments. This work was partly financed by FEDER funds through the Operational Programme Competitiveness Factors (COMPETE 2020) and by national funds through the Foundation for Science and Technology (FCT) within the scope of project SafEarth - PTDC/ECM-EST/2777/2014 (POCI-01-0145-FEDER-016737). The support from grants SFRH/BD/131006/2017 and SFRH/BPD/97082/2013 is also acknowledged.

References

1. Houben H, Guillaud H (2008) Earth construction: a comprehensive guide, CRATerre – EAG. Intermediate Technology Publication, London
2. Minke G (2006) Building with earth, design and technology of a sustainable architecture. Birkhäuser – Publishers for Architecture, Basel, Berlin, Boston
3. Pollock S (1999) Ancient mesopotamia. Cambridge University Press, Cambridge
4. Pacheco-Torgal F, Jalali S (2012) Earth construction: lessons from the past for future eco-efficient construction. Constr Build Mater 29:512–519
5. Jaquim PA, Augarde CE, Gerrard CM (2008) A chronological description of the spatial development of rammed earth techniques. Int J Archit Herit 2:377–400
6. Jaquin PA (2008) Analysis of historic rammed earth construction. Ph.D. thesis. Durham University, United Kingdom
7. Fernandes M (2013) A Taipa no Mundo. (C. d. Porto, Ed.) DigitAR, vol 1, pp 14–21
8. Bui TT, Bui QB, Limam A et al (2014) Failure of rammed earth walls: from observations to quantifications. Constr Build Mater 51:295–302
9. De Felice G, De Santis S, Garmendia L et al (2014) Mortar-based systems for externally bonded strengthening of masonry. Mater Struct 47:2021–2037
10. Ghiassi B, Marcari G, Oliveira DV et al (2012) Numerical analysis of bond behavior between masonry bricks and composite materials. Eng Struct 43:210–220
11. Valluzzi MR, Modena C, De Felice G (2014) Current practice and open issues in strengthening historical buildings with composites. Mater Struct 47:1971–1985
12. Borri A, Corradi M (2001) FRP: Fiber Reinforced Polymers. I materiali innovativi nell' edilizia e nel restauro. Recupero e Conservazione. De Lettera, Milano
13. Noguez R, Navarro S (2005) Reparación de muros de adobe com el uso de mallas sintéticas. In: PUCP, international conference SismoAdobe 2005. (in Spanish)
14. Torrealva D (2016) Static and dynamic testing for validating the polymer grid as external reinforcement in earthen buildings. In: Brick and block masonry: proceedings of the 16th international brick and block masonry conference, 26–30 June, Padova, Italy

15. Figueiredo A, Varum H, Costa A et al (2013) Seismic retrofitting solution of an adobe masonry wall. Mater Struct 46:203–219
16. Fagone M, Loccarini F, Ranocchiai G (2017) Strength evaluation of jute fabric for the reinforcement of rammed earth structures. Compos Part B Eng 133:1–13
17. Van Balen K, Papayianni I, Van Hees R et al (2005) Introduction to requirements for and functions and properties of repair mortars. RILEM TC 167-COM: 'Characterisation of Old Mortars with Respect to their Repair'. Mater Struct 38:781–785
18. Silva R (2013) Repair of earth constructions by means of grout injection. Ph.D. thesis, Department of Civil Engineering, Universidade do Minho, Guimarães, Portugal
19. Gomes MI, Faria P, Gonçalvez TD (2013) The compatibility of earth-based repair mortars with rammed earth substrates. In: 3rd historic mortars conference, Glasgow, Scotland
20. CEN (1999) Methods for test for mortar for masonry. Determination of flexural and compressive strength of hardened mortar EN 1015-11
21. Bui QB, Morel JC (2009) Assessing the anisotropy of rammed earth. Constr Build Mater 23:3005–3011
22. Silva RA, Oliveira DV, Schueremans L, et al (2014) Modelling the structural behaviour of rammed earth components. In: Topping BHV, Iványi P (eds) 12th international conference on computational structures technology. Civil-Comp Press
23. Miccoli L, Müller U, Fontana P (2014) Mechanical behaviour of earthen materials: a comparison between earth block masonry, rammed earth and cob. Constr Build Mater 61:327–339
24. Miccoli L, Oliveira DV, Silva RA et al (2015) Static behaviour of rammed earth: experimental testing and finite element modelling. Mater Struct 48:3443–3456
25. ISO3374 (2000) Reinforcement products. Mats and fabrics. Determination of mass per unit area
26. ASTM (2015) Standard test method for determining tensile properties of geogrids by the single or multi-rib tensile method D6637
27. De Felice G, Aiello MA, Caggegi C, et al (in press) Test method to characterize the Textile Reinforced Mortar to substrate bond, Recommendation of RILEM Technical Committee 250-CSM: Composites for Sustainable Strengthening of Masonry